JOM, Vol. 75, No. 4, 2023
https://doi.org/10.1007/s11837-022-05574-9

Effect and Mechanism of Acetic Acid to Improve the Hydration Activity of Steel Slag

GANGZHE CHEN,[1,2] SIYUAN BIAN,[1,2] JIAN GAO,[1,2] PENG JIN,[1,2] and RUIXING WANG [1,2,3]

1.—College of Materials Science and Engineering, Southeast University, Nanjing 211189, China. 2.—Jiangsu Key Laboratory of Construction Materials, Southeast University, Nanjing 211189, China. 3.—e-mail: ruixing@seu.edu.cn

We found that acetic acid could activate the hydration properties of steel slag powder to a certain extent and improve its strength. Minerals in steel slag, such as $Mg_2Al(OH)_7$, f-CaO, C_3S, C_2S, C_2F, and RO phases, could be dissolved by acetic acid, leaching more Ca^{2+} to participate in the hydration process. The major hydration products were silica gel and calcium silicate hydrate (C-S-H) gel. With the increase of acetic acid concentration, the size of hydration products increased, and the total porosity reduced. However, if the concentration was too high, more H^+ reacted with the carbonate and iron in the steel slag, generating more CO_2 and H_2, and producing more air pores in the steel slag paste. Activated by 3 mol/L acetic acid, the 3-day, 7-day, and 28-day compressive strengths of the steel slag compacts could reach 36.3 MPa, 44.6 MPa, and 51.9 MPa, which was much higher than the control group.

INTRODUCTION

Steel slag is one of the main solid wastes generated during the steelmaking process. In China, the production of steel slag has exceeded 110 million tons per year but the utilization is still less than 30%.[1,2] Most of the unused steel slag is landfilled, resulting in a series of environmental and ecological problems.[3,4]

As the composition is similar to cement, steel slag can be used as a cementitious material and mineral admixture.[5] C_2S, C_3S, C_2F, and RO phase (FeO–MnO–MgO solid solution) are the main minerals. But low hydration activity and poor volume stability limit the scope of steel slag application, resulting in it having little value.[6–10]

Alkali activation is the most common way to enhance the hydration properties of solid wastes, including steel slag.[5] It can not only recycle solid wastes but also reduce the amount of cement, cutting the cost and carbon emissions.[11] Up to now, alkali-activated steel slag has been widely used in mortar,[12,13] concrete,[14] brick,[15] and secondary aggregates.[16] But the RO phase in steel slag is hydration inert, and alkali activators cannot improve its activity.[17]

Using an acid as an activator seems to be a good choice to overcome the deficiencies of the alkali-steel slag system. Acids can promote the dissolution of RO phases, Ca/Mg-bearing silicates, and $Ca(OH)_2$.[18–20] At present, acid has played an important role in the utilization of steel slag;[21] improving calcium leaching from steel slag to absorb CO_2 is a common use, like CaO-based sorbent making[22] and $CaCO_3$ production.[23] Compared with strong acids, the extraction efficiency of organic acids for elements in steel slag is higher.[24] There are few studies on the use of acid to improve the hydration activity of steel slag. Compared with steam curing and alkali activation approaches, Huo et al. pointed out that surface modification by acid was a low energy consumption approach to enhance the hydration activity and soundness properties of steel slag, especially acetic acid (HAc) for more beneficial to improve the long-term performances.[25] But they focused on the modification of steel slag powders by glacial acetic acid-anhydrous alcohol solution. On the one hand, this modification contributes less to increases in strength, especially 28-day strength.

(Received August 15, 2022; accepted October 12, 2022; published online November 9, 2022)

On the other hand, the flammability of anhydrous alcohol limits its utilization in industrial production.

In this paper, acetic acid was used as the activator directly and the change of hydration activity of the steel slag was investigated, aiming to offer a new technique for steel slag utilization. The concentration range of the acetic acid was 1–6 mol/L, and the optimal concentration of acetic acid was determined by compressive strength, the heat of hydration, changes in mineral composition, microscopic morphology, and pore structure.

MATERIALS AND METHODS

Raw Material

The steel slag was produced by Taigang Iron & Steel Group Corp., Shanxi, China. The diameter of steel slag powders was less than 80 μm. The chemical compositions determined by x-ray fluorescence (XRF) are shown in Table I. The mineral composition was found by x-ray diffraction (XRD) analysis and is presented in Fig. 1a. The main minerals in steel slag are C_2S, C_3S, C_2F, C_3A, and RO phase. It could be observed by scanning electron microscope (SEM) that the steel slag powder had high crystallinity and an irregular shape (Fig. 1b).

The purity of the acetic acid was AR, and it was produced by Shanghai Lingfeng Chemical Reagent Co., Ltd. The acetic acid solutions of different concentrations were prepared with deionized water.

Preparation of Samples

Cylindrical steel slag compacts with a diameter of 20 mm and a height of 20 mm were prepared. They were made by mixing 15 g steel slag powder with 1.8 g deionized water or acetic acid solution, stirring for 120 s, and putting 15.5 g of mixture into the mold, applying a pressure of 8 MPa, and maintaining this for 120 s. After demolding, the specimens were cured under a relative humidity higher than 60% at 20 °C. The curing times were 1 day, 3 days, 7 days, and 28 days.

To ascertain the dissolution mechanism of acetic acid on steel slag, mixed acetic acid and steel slag, in a weight ratio of 2:1, was left for 72 h for observation and to analyze the mineral composition changes of residues after filtering.

Test Methods

The compressive strength was calculated according to the Chinese standard: GB/T 50,107 standard for evaluation of concrete compressive strength. Three specimens were measured in each group with a loading rate of 0.6 kN/s.

The hydration heat was measured by an isothermal calorimeter (TAM AIR), and the initial temperature was 20 °C. The temperature of steel slag paste in the mixing process was measured by a handheld thermometer.

The Ca^{2+} leaching properties and pH value of the steel slag paste were measured. The steps were as follows. First, 10 g of steel slag was mixed with 1.2 g water or acetic acid solution, stirred for 120 s, and rested for 0.5 h or 20 h. Then, 1.12 g of the mixture was put into 10 g deionized water, stirred for 300 s, and filtered. The pH value of the filtrate was measured with a pH meter (PHS-3E) and the leaching of calcium was measured by the EDTA titration method.[26]

The mineral composition was found by using a D8-Discover x-ray diffractometer (XRD) with Cu K_α radiation (30 kV and 30 mA, scan interval 5–70° 2 theta, 0.02° and 0.15 s/step). Quantitative x-ray diffraction analysis (QXRD) was also used for analysis. Compared with XRD, the scanning speed was 0.3 s/step, adding 10 wt.% of corundum (α-Al_2O_3) as an internal standard into samples. Fourier IR spectroscopy (FT-IR, Nicolet iS10) was also used to analyze the functional groups with a testing range of 4000–400 cm^{-1}. Scanning electron microscopy (SEM) was achieved by a field emission environment scanning electron microscope (FEI 3D) with an energy-dispersive x-ray analyzer.

Porosity and pore structure were characterized by mercury intrusion porosimetry (MIP) (Auto pore IV 9520). The highest pressure was 30,000 psi and accuracy was better than 0.05%.

RESULTS AND DISCUSSION

Compressive Strength

The specimens were named H0, H1, H2, H3, H4, H5, and H6, as seen in Table II.

The compressive strength of the steel slag at different ages is shown in Fig. 2. It was clear that using acetic acid as an activator could improve the strength of compacts. After 1 day, with the increase of acetic acid concentration, the number of H^+ increased, and the dissolution and hydration of alkaline minerals in the steel slag were more rapid. After curing for 3 days, the compressive strength of the steel slag specimens gradually increased, with the concentration increasing to 1–3 mol/L. When the concentration was increased to 6 mol/L, the excess concentration of acetic acid had a negative effect on the hydration reaction, and the

Table I. The chemical composition of the steel slag

Compound	CaO	Fe_2O_3	SiO_2	MgO	MnO	Al_2O_3	P_2O_5	TiO_2	SO_3	Other
wt.%	33.63	27.66	18.25	5.92	4.66	3.86	2.03	0.96	0.76	2.27

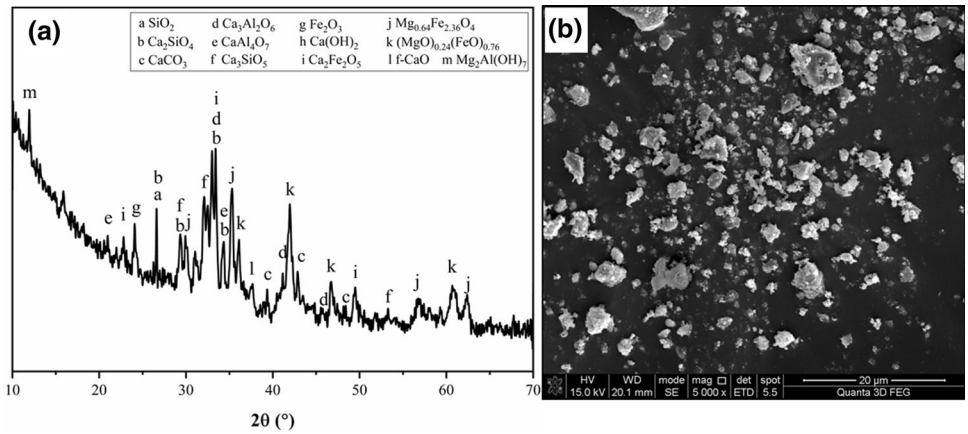

Fig. 1. Steel slag powder: (a) XRD pattern; (b) micromorphology.

Table II. The mixture ratio design of the steel slag compacts

Number	Concentration of HAc (mol/L)	Weight of steel slag powder (g)	Weight of HAc solution (g)
H0	0	15.0	1.8
H1	1	15.0	1.8
H2	2	15.0	1.8
H3	3	15.0	1.8
H4	4	15.0	1.8
H5	5	15.0	1.8
H6	6	15.0	1.8

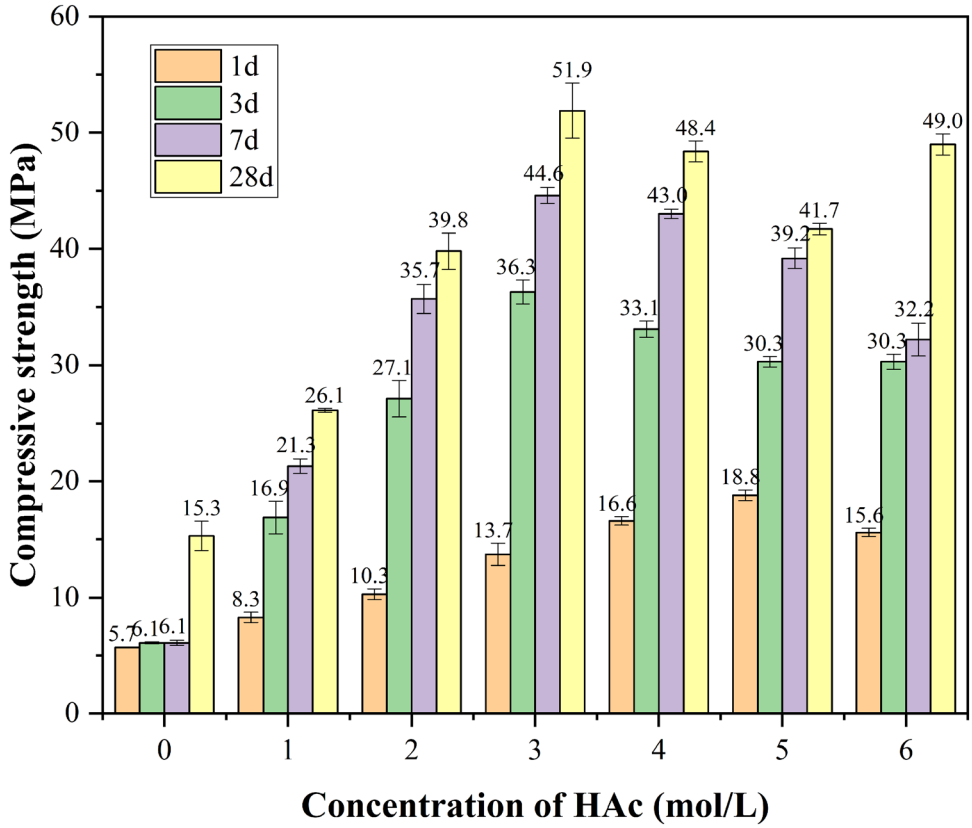

Fig. 2. The compressive strength of the steel slag.

compressive strength showed a slight decrease, although it was still higher than that of the control (H0). Therefore, the optimal concentration was 3 mol/L in this test.

Hydration Heat and Ca^{2+} Leaching

In the process of mixing, the addition of acetic acid would increase the temperature in the steel slag paste. The higher the concentration, the more heat was released, as shown in Fig. 3. Figure 3a shows the maximum temperature during the mixing process, while Fig. 3b was the result of the hydration heat.

Usually, the curve of a cement-based material's hydration heat includes 2 exothermic peaks with five hydration stages: dissolution stage (the first peak), induction stage, acceleration stage (the second peak), deceleration stage, and low reaction stage.[27] Compared with cement, only a fast and short-term exothermic peak could be found in the curve of steel slag (Fig. 3b), consistent with Gu's result.[28] Contacting with water, a little energy on the surface of the steel slag powder was released without acetic acid, resulting in this exothermic peak. Activated by acid, the heat evolution became greater, which was possible because of the mineral's dissolution and hydration. An anomalous exothermic peak could be found in the group of 1 mol/L acetic acid within 4–6 h, which may be due to the gradual dissolution of alkaline minerals. Although the effect of 1 mol/L acetic acid is not as obvious as that of higher concentrations in short order, hydrogen ions still played a certain role in dissolution and hydration, which may lead to anomalous exothermic peak.

As for the acceleration of the cement, the hydration of C_3S became rapid with C-S-H gels and $Ca(OH)_2$ formation.[29] As the C_3S content was less in steel slag, the second exothermic peak of water specimens was not clear. H^+ offered by acetic acid might reduce the production of $Ca(OH)_2$, so the inconspicuous second exothermic peak might be the result of gel growth.

Dissolution of minerals in steel slag by acetic acid was a reason for the release of heat. The most abundant metal element in steel slag was Ca, which was an important component of hydration products. The leaching characteristics of Ca from steel slag with different concentrations of acetic acid were studied, and the results can be seen in Fig. 4. The leaching times were 0.5 h (Fig. 4a) and 20 h (Fig. 4-b), corresponding to the end of the dissolution stage and acceleration stage, respectively. With the increase of acetic acid concentration, the amount of calcium leaching increased. Comparing the two results, it can be seen that when the concentration was less than 3 mol/L, the leaching amount of Ca in 20 h was lower than that in 0.5 h, which meant that the consolidation rate was higher than the leaching rate. When the concentration was higher than 3 mol/L, the opposite occurred. The Ca reached an equilibrium of consolidation and dissolution in the steel slag specimen activated by 3 mol/L acetic acid.

The change in pH value followed the same rules. When the leaching time was 0.5 h, the reaction between acid and steel slag was incomplete and the pH of the paste was related to the amount of H^+ that the acetic acid could provide; the higher the concentration, the lower the value. As the reaction progressed, the difference in the solubility of the minerals at different concentrations was reflected. Low concentration acetic acid solutions dissolved Ca selectively while high concentrations dissolved most of the Ca in the steel slag minerals.[23,30] Most alkaline minerals cannot be dissolved in a weak acid. As the concentration increased, more minerals were dissolved, releasing more OH^-, so that the pH value became higher. If the concentration exceeded 3 mol/L, excess H^+ decreased the pH value again.

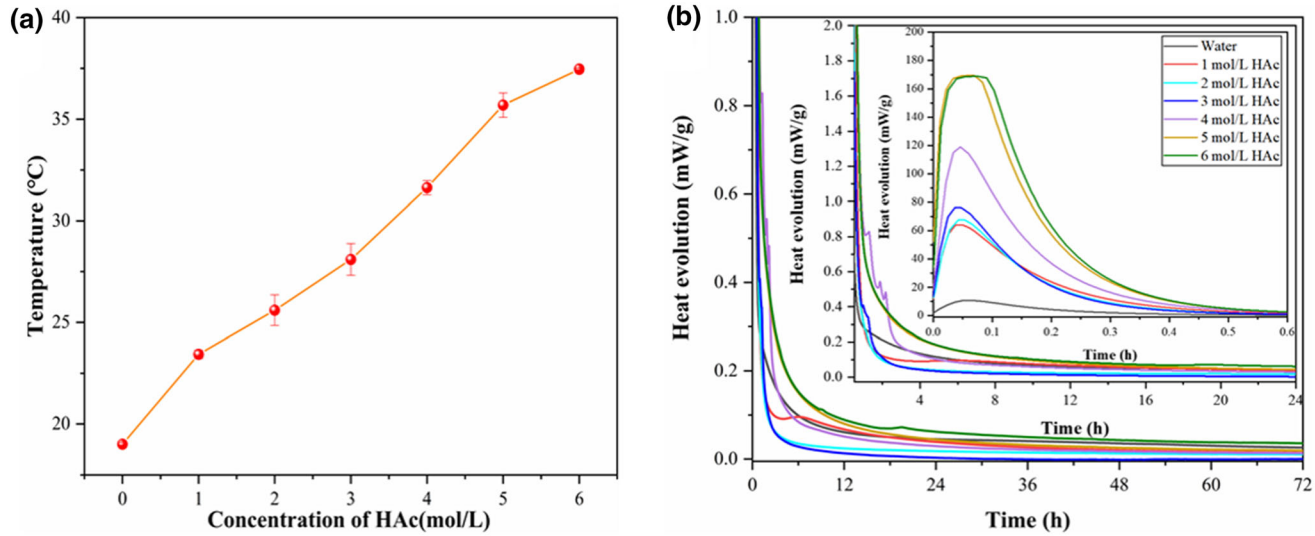

Fig. 3. Heat release of steel slag paste: (a) maximum temperature inside during mixing; (b) hydration heat.

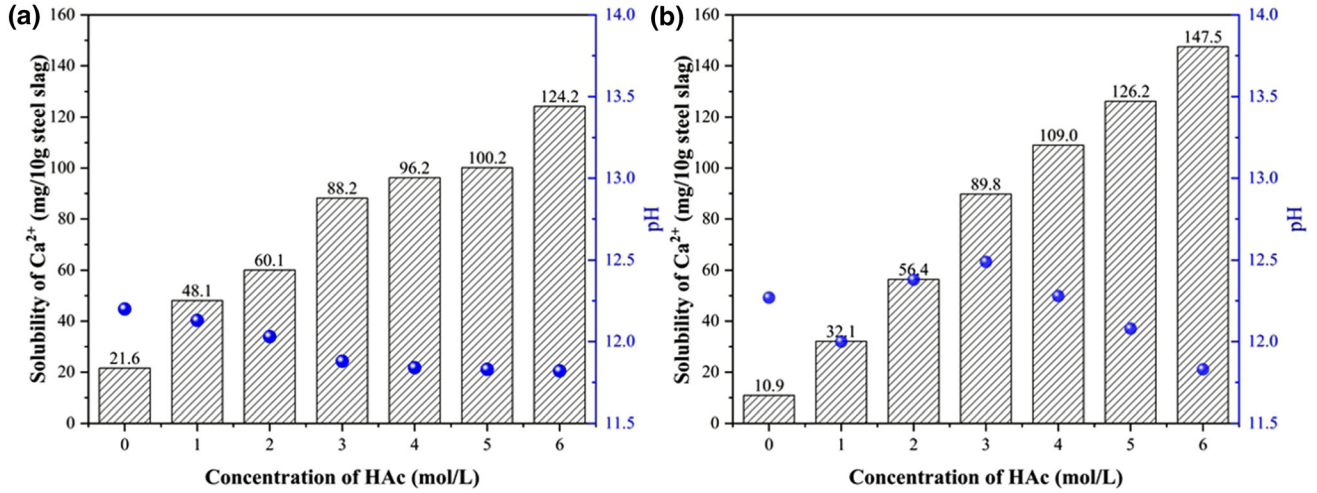

Fig. 4. The leaching of calcium and pH values: (a) 0.5 h; (b) 20 h.

Mineral Composition and Microstructure of Steel Slag Specimens

Mineral Composition

Figure 5 displays the XRD and FT-IR of steel slag samples reacted with different concentrations of acetic acid at 3 days and 28 days. According to the XRD results at 3 days (Fig. 5a), it was clear that the peak of $Mg_2Al(OH)_7$ disappeared, which meant that acetic acid promoted the dissolution of the mineral at an early stage. Besides, C_3S, C_2S, C_3A, C_2F, and RO phases reacted with acetic acid, so their characteristic peaks decreased. Moreover, f-CaO cannot be found in the samples activated by acid, increasing the volume stability.

However, new crystalline minerals were not found, and the difference between the samples activated by acid was inconspicuous. Thus, only H0, H1, H3, and H6 samples continued to be analyzed. Compared with the XRD results at 3 days, the peak of $Mg_2Al(OH)_7$ decreased in H0 at 28 days (Fig. 5b). The hydration products were probably dominated by the amorphous phase, so the differences cannot be judged by XRD. FT-IR was used to determine the type of functional group. The result at 28 days is shown in Fig. 5c. The appearances of the bands near 3451 cm^{-1}, 2830 cm^{-1}, 2718 cm^{-1}, and 1598 cm^{-1} could be attributed to the H-O-H of H_2O while 1416 cm^{-1} could be attributed to the C-O stretching vibrations in CH_3COO^- or CO_3^{2-}. The absorption band at around 1097 was the Si-O bond vibration (v_3) in silica gels.[31] The band at a frequency of 875 cm^{-1} corresponded to carbonate C-O stretching vibrations (v_2) in CO_3^{2-} and 775 was also the Si–O bond (v_4) of calcium silicate hydrate (xCaO·ySiO$_2$·H$_2$O, C-S-H) gels,[32] a common amorphous hydration product of cement-based materials. Intuitively, the types of hydration products were basically the same, including silica gels and C-S-H gels. Thus, the amount and the morphology of hydration products might be the most critical factors affecting strength.

Because of various minerals in steel slag, peaks overlap each other, which makes it more difficult to analyze the effect of acetic acid. Meanwhile, the peaks of several hydration products, like calcium acetate, could not be clearly found. Thus, the effect of concentrations of acetic acid on mineral dissolution and hydration products in steel slag was further analyzed by increasing acetic acid consumption. The results are shown in Fig. 6.

As soon as the steel slag and the acetic acid solution came into contact, air pores were generated, resulting from H^+ reacting with $CaCO_3$ or Fe.

$$CaCO_3 + 2CH_3COOH \rightarrow Ca(CH_3COO)_2 + CO_2 + H_2O \quad (1)$$

$$Fe + 2CH_3COOH \rightarrow Fe(CH_3COO)_2 + H_2 \quad (2)$$

When dissolved by 6 mol/L HAc, steel slag paste lost fluidity within 5 min, so many air pores remained in the paste. After standing for 72 h, with an increase of concentration of the HAc, the volume of the liquid supernatant reduced. QXRD was used to measure the number of hydration products and the consumption of minerals in steel slag residue after it had been filtered and dried, as shown in Fig. 7.

The excess acetic acid made the analysis clearer and easier. As Fig. 7a shows, the peak of calcium acetate [$Ca(CH_3COO)_2$, $Ca(Ac)_2$] could be found. Moreover, ettringite and $Mg_6Al_2(CO_3)(OH)_{16}{\cdot}4H_2O$ showed up in 3 mol/L groups. The proportion of C_3S, C_2S, C_2F, FeO, and RO phases was significantly reduced, especially C_3S, and α-C_2S, which were reacted with 6 mol/L acid completely (Fig. 7b and c).

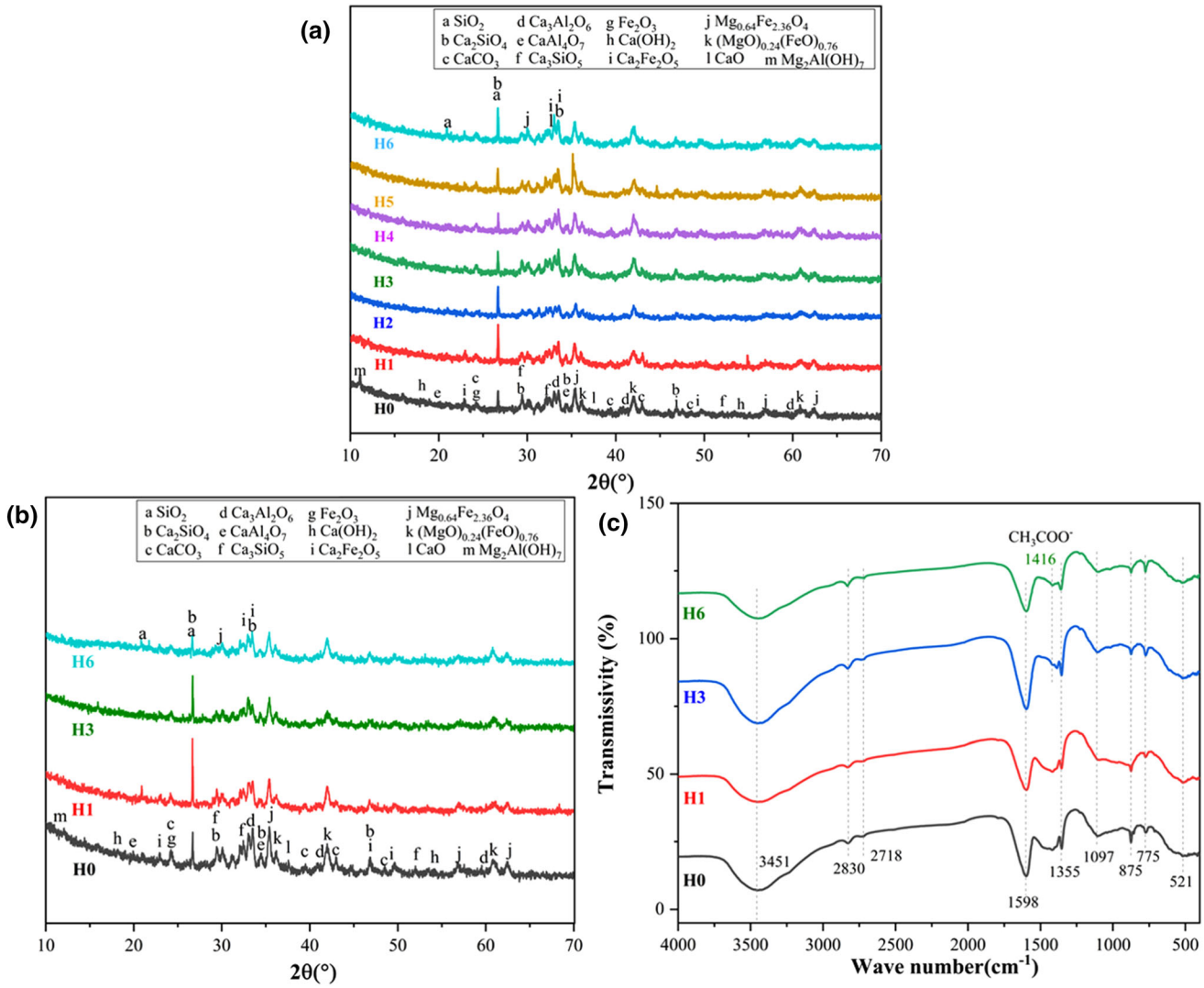

Fig. 5. Mineral composition of steel slag compacts: (a) XRD at 3 days; (b) XRD at 28 days; (c) FT-IR at 28 days.

$$Ca_3SiO_5 + 6CH_3COOH \rightarrow 3Ca^{2+} + 6CH_3COO^- + SiO_2 + 3H_2O \quad (3)$$

$$Ca_2SiO_4 + 4CH_3COOH \rightarrow 2Ca^{2+} + 4CH_3COO^- + SiO_2 + 2H_2O \quad (4)$$

$$CaO + 2CH_3COOH \rightarrow Ca^{2+} + 2CH_3COO^- + 2H_2O \quad (5)$$

$$Ca_2Fe_2O_5 + 4CH_3COO \rightarrow 2Ca^{2+} + 4CH_3COO^- + Fe_2O_3 + 2H_2O \quad (6)$$

$$FeO + 2CH_3COOH \rightarrow Fe^{2+} + 2CH_3COO^- + H_2O \quad (7)$$

Meanwhile, compared with H0, amorphous substances (C-S-H gel and silica gels) increased, which confirmed that acetic acid played a positive role in hydration. Interestingly, when the acetic acid concentration was excessive, most of the Ca^{2+} in the steel slag combined with the CH_3COO^- to form calcium acetate, while the amorphous Ca^{2+} disappeared because of decalcification in acid solutions.[33]

$$C\text{-}S\text{-}H + CH_3COOH + H_2O \rightarrow Ca(CH_3COO)_2{\cdot}H_2O + Si^{4+} + CH_3COO^- \quad (8)$$

Finally, the QXRD analysis of H0 and H3 at 28 days is shown in Fig. 7d. The changing trend of minerals was the same as that in Fig. 7b, but the amount of change was slightly lower.

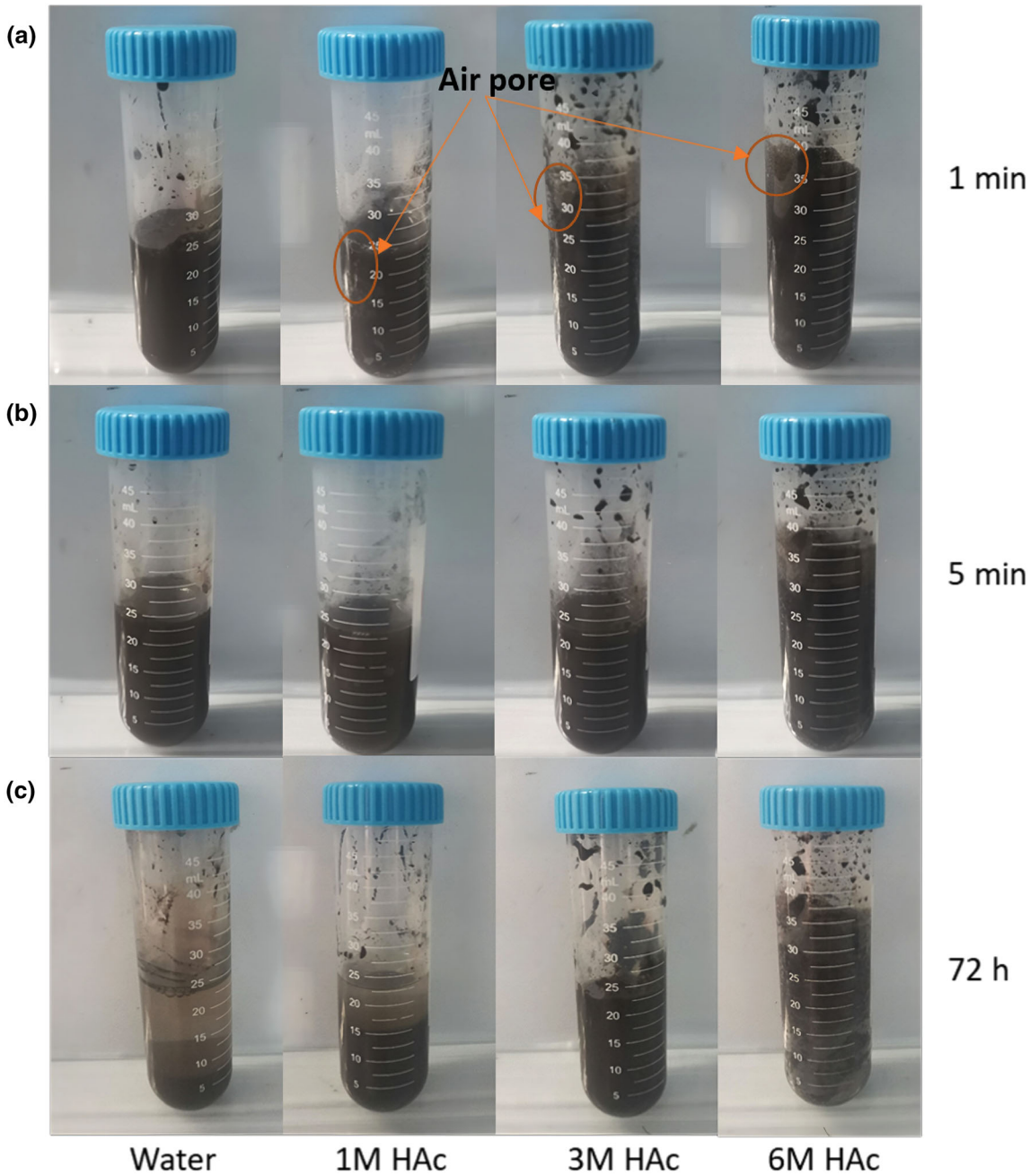

Fig. 6. Observations of steel slag paste dissolved by acetic acid solutions of different strengths.

Microstructure

QXRD verified the increase in the number of hydration products, while the micromorphology of the samples at 28 days was observed by SEM, as shown in Fig. 8. The size of the hydration products in H0 and H1 were less than 1 μm, loosely depositing on the surface of the steel slag so that the compressive strength was low. The structure of the hydration products in H3 and H6 were more compact, and larger. It is worth noting that a penetrating and obvious crack could be found in H6. Drying shrinkage caused by excessive heat release in the early stage might be one of the reasons for cracks. Meanwhile, after contact with water in the environment, white crystals would precipitate on the surface of the sample (Fig. 8i). These were found to be $Ca(CH_3COO)_2$ after analyzing with XRD (Fig. 8j). The process of ion migration also made the microstructure deteriorate.

Looking at the SEM images, the porosity and pore structures appeared to be different, and this could govern the strength of the steel slag. To investigate this, we measured pore structures precisely using MIP. According to diameter, the pores of cement-based materials could be divided into 4 types: gel

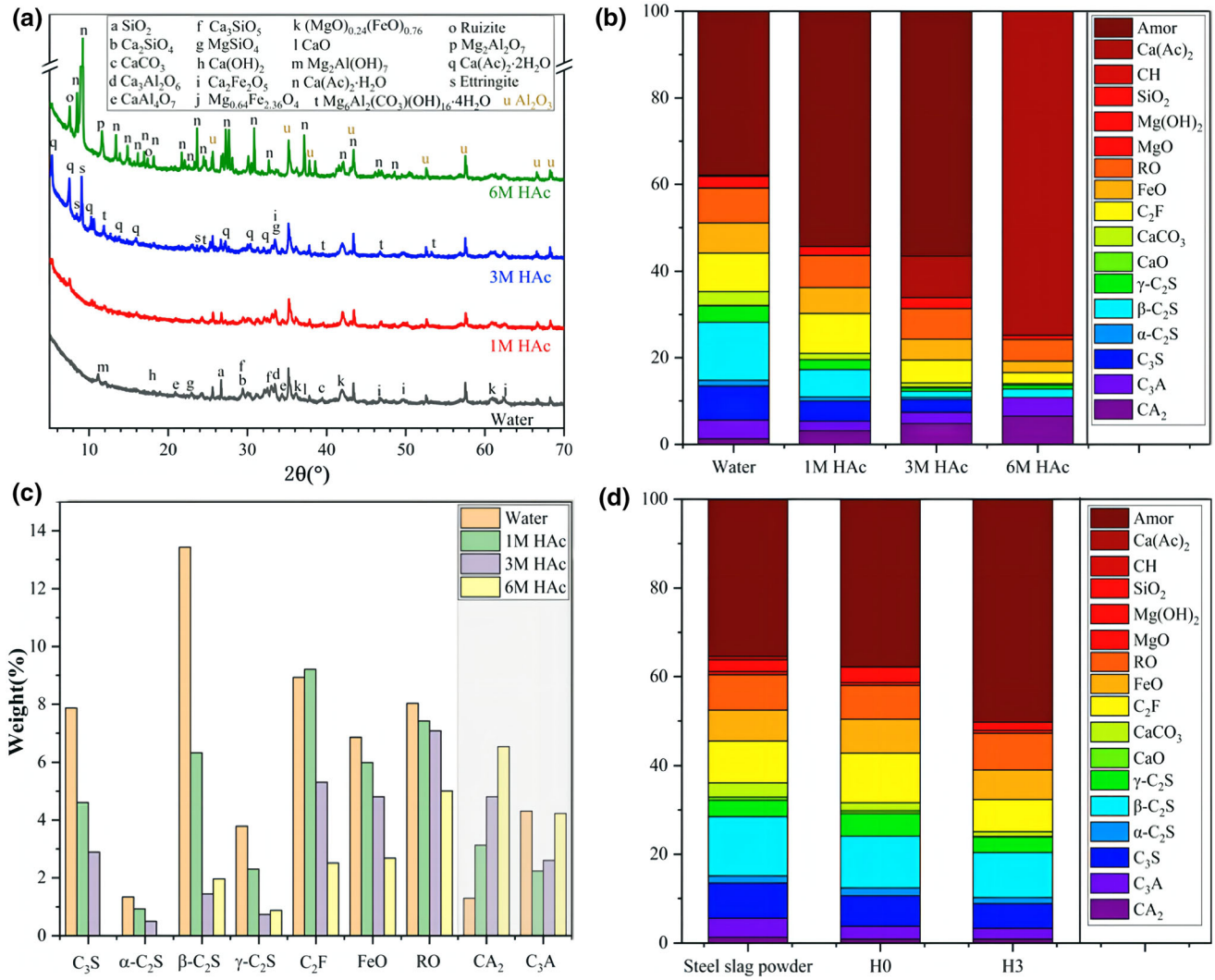

Fig. 7. QXRD analysis. (a) XRD pattern; (b) QXRD analysis results of residue; (**c**) main minerals changing in residue; (**d**) QXRD analysis results of compacts at 28 days.

pores (< 10 nm), medium capillary pores (10–50 nm), large capillary pores (50 nm–1 μm), and macro pores (> 1 μm).[34] Pores over 10 nm in diameter might influence the strength,[35] and the larger the diameter of the pore, the greater the effect on strength. The analysis of MIP results based on this concept is shown in Fig. 9. Figure 9a shows the effect of acetic acid concentration on pore diameter distribution, and Fig. 9b shows the proportions of each kind of pore. Acetic acid reduced the porosity of the compacts. The total porosity decreases with increasing acetic acid concentration. The total porosity of H1 was basically consistent with H0. With increasing concentration, medium capillary pores, large capillary pores, and macro pores decreased, resulting in a reduction in total porosity. It should be noted that acetic acid released heat and created bubbles in the process of dissolving steel slag so that air pores could be found in both H1 and H6. The micro-cracks created by ion migration also created air pores. As for H3, in theory, there should be air pores in it, too. But more hydration products filled the air pores (Figs. 6 and 7).

Factors that affected strength included large capillary pores, macro pores, and porosity.[34] Although the porosity of H3 was a little higher than H6, because H3 didn't have air pores, the strength was the highest out of all the samples.

CONCLUSION

This work investigated the effects and mechanism of acetic acid to improve the hydration activity of steel slag. The conclusions are as follows.

(1) Acetic acid plays an effective and efficient role in the steel slag hydration process, and 3 mol/L was a suitable concentration. A lower concentration cannot completely activate the hydration activity of steel slag. A higher concentration might cause micro-cracks and air pores because of drying shrinkage and ion migration.

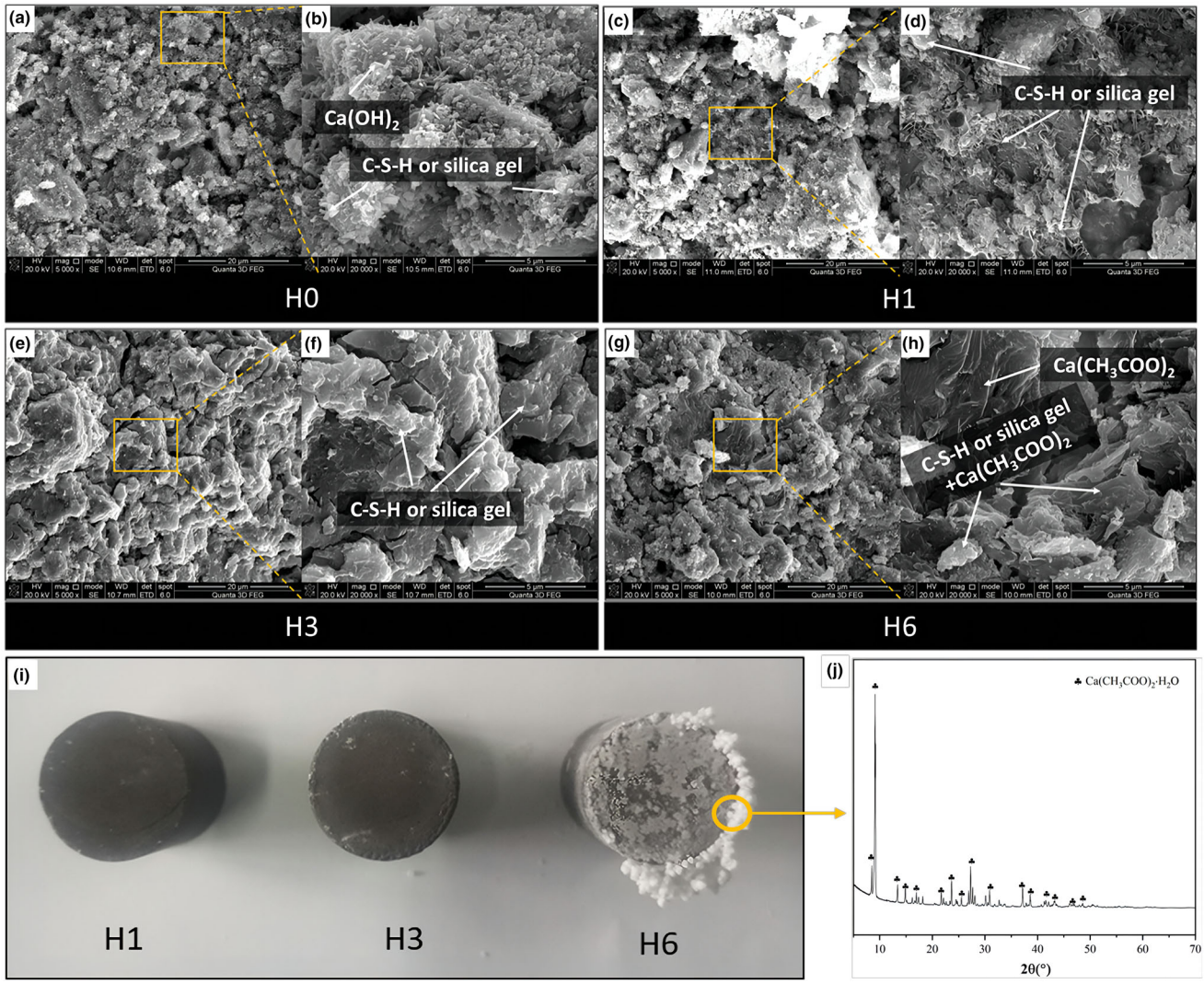

Fig. 8. SEM images of steel slag samples at 28 days (a–h). (i) Photograph showing samples with white crystals on H6; (j) XRD of white crystals showing that they were $Ca(CH_3COO)_2$.

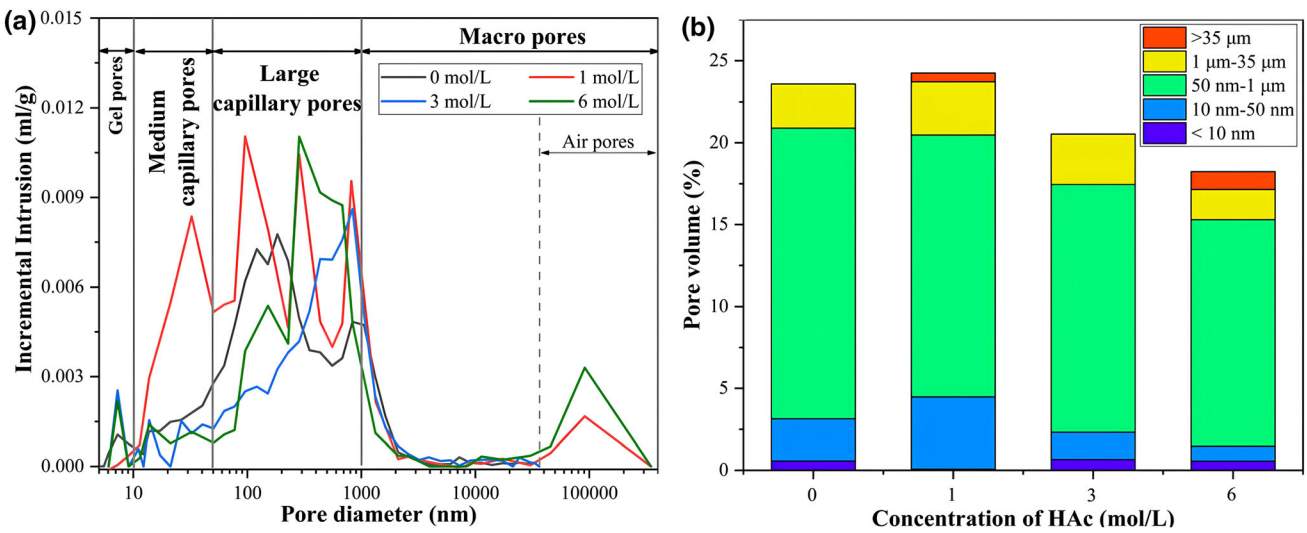

Fig. 9. MIP results of steel slag compacts: (a) effect of acetic acid concentration on pore diameter distribution; (b) effect of acetic acid concentration on pore volume.

(2) Acetic acid promotes the dissolution of minerals in steel slag, such as f-CaO, C_3S, C_2S, C_3A, C_2F, and RO phases and leaching Ca^{2+} with heat release.
(3) Amorphous silica gel and C-S-H gel are the main hydration products. As the concentration of acetic acid is increased, there is no significant change in the type of hydration products. Change of morphology and increase of quantity and size of hydration products was the main reason for the increase in strength of the steel slag.

ACKNOWLEDGEMENTS

The authors appreciate the financial support from the National Nature Science Foundation of China (Grant No. 51872046).

CONFLICT OF INTEREST

The authors declare that they have no known competing financial interests or personal relationships that could have appeared to influence the work reported in this paper.

REFERENCES

1. Z. Liu, D.-W. Zhang, L. Li, J.-X. Wang, N.-N. Shao, and D.-M. Wang, *Constr. Build. Mater.* 204, 158 (2019).
2. Z. Chen, R. Li, X. Zheng, and J. Liu, *Cem. Concr. Res.* 139, 106271 (2021).
3. R. Baciocchi, G. Costa, A. Polettini, and R. Pomi, *J. Hazard. Mater.* 286, 369 (2015).
4. J. Guo, Y. Bao, and M. Wang, *Waste Manag.* 78, 318 (2018).
5. N. You, B. Li, R. Cao, J. Shi, C. Chen, and Y. Zhang, *Constr. Build. Mater.* 227, 116614 (2019).
6. J. Liu, C. Yi, H. Zhu, and H. Ma, *Materials* 12(20), 3307 (2019).
7. F. Sha, H. Li, D. Pan, H. Liu, and X.J. Zhang, Mater. *Res. Technol.* 9(3), 2793 (2020).
8. T.-T.-H. Nguyen, D.-H. Phan, H.-H. Mai, and D.-L. Nguyen, *Materials* 13(8), 1928 (2020).
9. S.R. Tonapa, L. Febriani, and D. Sandy, *IOP Conf. Ser. Earth Environ. Sci.* 473, 012142 (2020).
10. X. Li, K. Li, Q. Sun, L. Liu, J. Yang, and H. Xue, *Materials* 14(8), 2052 (2021).
11. J. Sun, Z. Zhang, S. Zhuang, and W. He, *Constr. Build. Mater.* 241, 118141 (2020).
12. N. You, J. Shi, and Y. Zhang, *Corros Sci.* 175, 108874 (2020).
13. N. Cristelo, J. Coelho, T. Miranda, Á. Palomo, and Á. Fernández-Jiménez, *Cem. Concr. Compos.* 103, 11 (2019).
14. J. Rosales, F. Agrela, J.L. Díaz-López, and M. Cabrera, *Materials* 14(14), 3945 (2021).
15. W.S. Zhang, D. Shi, Z.J. Shao, J.Y. Ye and Y. Wang, *The Properties of Steel Slag Bricks Prepared by Both Alkali Activation and Accelerated Carbonation.* Paper presented at 3rd Mainland, Taiwan and Hong Kong Conference on Green Building Materials, 509, 113 (2011).
16. M. Morone, G. Costa, E. Georgakopoulos, V. Manovic, S. Stendardo, and R. Baciocchi, *Waste Biomass Valoriz.* 8(5), 1381 (2017).
17. Q. Wang, and P. Yan, *Constr. Build. Mater.* 24(7), 1134 (2010).
18. X. Mei, Q. Zhao, Y. Min, C. Liu, H. Saxén, and R. Zevenhoven, *Process Saf. Environ. Prot.* 159, 221 (2022).
19. R. Ragipani, S. Bhattacharya, and A.K. Suresh, *Proc. R. Soc. A* 475(2224), 20180830 (2019).
20. H. Zhang, X.Y. Zhang, and H.M. Long, *Spectrosc. Spectral Anal.* 38(11), 3502 (2018).
21. B. Zhang, Y. Chen, B. Zhang, R. Peng, Q. Lu, W. Yan, B. Yu, F. Liu, and J. Zhang, *Renew. Energy* 184, 592 (2022).
22. S. Tian, J. Jiang, F. Yan, K. Li, and X. Chen, *Environ. Sci. Technol.* 49(12), 7464 (2015).
23. S. Teir, S. Eloneva, C.-J. Fogelholm, and R. Zevenhoven, *Energy* 32(4), 528 (2007).
24. S. Hong, H.D. Huang, G. Rim, Y. Park, and A.-H.A. Park, *ACS Sustain. Chem. Eng.* 8(50), 18519 (2020).
25. B. Huo, B. Li, C. Chen, Y. Zhang, and D. Wang, *Constr. Build. Mater.* 307, 125004 (2021).
26. M. o. E. a. E. o. t. P. s. R. o. China, GB 7476-87 (1987).
27. L. Liu, P. Yang, B. Zhang, C. Huan, L. Guo, Q. Yang, and K.-I. Song, *Constr. Build. Mater.* 272, 121827 (2021).
28. Y. Gu, Y. Zhang, J. Chang, T. Zhang, and C. Shi, *J. Sustain. Cem. Based Mater.* 10(1), 46 (2021).
29. F. Han, R. Liu, D. Wang, and P. Yan, *Thermochim. Acta* 586, 52 (2014).
30. S. Eloneva, S. Teir, J. Salminen, C.-J. Fogelholm, and R. Zevenhoven, *Ind. Eng. Chem. Res.* 47(18), 7104 (2008).
31. B. Lu, C. Shi, J. Zhang, and J. Wang, *Constr. Build. Mater.* 186, 699 (2018).
32. I. García-Lodeiro, A. Fernández-Jiménez, M.T. Blanco, and A. Palomo, *J. Sol-Gel Sci. Technol.* 45(1), 63 (2008).
33. T. Damion, R. Cepuritis, and P. Chaunsali, *Cem. Concr. Compos.* 130, 104524 (2022).
34. S. Wang, Z. Wang, T. Huang, P. Wang, and G. Zhang, *Constr. Build. Mater.* 314, 125683 (2022).
35. D.A. Silva, V.M. John, J.L.D. Ribeiro, and H.R. Cem, *Concr. Res.* 31(8), 1177 (2001).